A method of strategic evaluation of energy performance of Building Integrated Photovoltaic in the urban context

Journal of Cleaner Production 184 (2018) 82–91

Contents lists available at ScienceDirect

Journal of Cleaner Production

journal homepage: www.elsevier.com/locate/jclepro

A method of strategic evaluation of energy performance of Building Integrated Photovoltaic in the urban context

V. Costanzo [a], R. Yao [a, *], E. Essah [a], L. Shao [a], M. Shahrestani [a], A.C. Oliveira [b], M. Araz [c], A. Hepbasli [c], E. Biyik [c]

[a] School of the Built Environment, University of Reading, RG6 6AW, Reading, UK
[b] Centre for Renewable Energy Research, University of Porto, 4200-465, Porto, Portugal
[c] Department of Energy Systems Engineering, Faculty of Engineering, Yasar University, 35100, Izmir, Turkey

ARTICLE INFO

Article history:
Received 24 November 2017
Received in revised form
2 February 2018
Accepted 13 February 2018
Available online 23 February 2018

Keywords:
Solar potential
Urban modelling
BIPV
Energy matching
Energy supply and demand

ABSTRACT

This paper presents an integrated bottom-up approach aimed at helping those dealing with strategical analysis of installation of Building Integrated Photo Voltaic (BIPV) to estimate the electricity production potential along with the energy needs of urban buildings at the district scale. On the demand side, hourly energy profiles are generated using dynamic building simulation taking into account actual urban morphologies. On the supply side, electricity generated from the system is predicted considering both the direct and indirect components of solar radiation as well as local climate variables. Python-based Algorithm editor Grasshopper is used to interlink four types of modelling and simulation tools as 1) generation of 3-D model, 2) solar radiation analysis, 3) formatting weather files (TMY data set) and 4) dynamic energy demand. The method has been demonstrated for a cluster of 20 buildings located in the Yasar University in Izmir (Turkey), for which it is found the BIPV system could achieve an annual renewable share of 23%, in line with the Renewable Energy Directive target of 20%. Quantitatively-compared demand and supply information at hourly time step shows that only some energy needs can be met by BIPV, so there is a need for an appropriate matching strategy to better exploit the renewable energy potential.

1. Introduction

In the past years, EU Commission put into force the recast version of the Directive on the Energy Performance of Buildings (EU, 2010) and the Renewable Energy Directive (European Parliament, 2009) to achieve the targets of: i) reducing greenhouse gas emissions of 20% relative to 1990 levels, ii) improving the energy efficiency of buildings up to 20% and iii) increase the share of renewable energy to 20%. All these objectives have to be met by 2020. In EU countries, there are more than 160 million buildings accounting for almost 40% of primary energy consumption and most of them have been built when no energy efficiency regulations were into force (iNSPiRe Projects, 2014), so there is a space for renewable and sustainable energy generation technologies to rapidly spread. Within this context, photovoltaic (PV) technology is growing quickly compared to other renewables, and Building Integrated Photo Voltaic (BIPV) in particular. In fact, apart from producing clean energy directly on-site, architectural integration to roofs and walls may add additional benefits such as reduced costs of material and labour and improved aesthetic (Baljit et al., 2016).

A recent review paper about BIPV systems (Biyik et al., 2017) categorized the existing literature into 5 different groups: i) building-scale applications and experimental studies, ii) building-scale simulation and numerical studies, iii) cell/module design studies, iv) grid integration studies and v) policy and strategies studies.

If looking at studies about the use of BIPV panels at district/urban scales, most of the authors focused on the estimate of the solar potential of roofs and facades following two main approaches: the use of Digital Surface Models (DSM) and of Laser Imaging Detection and Ranging (LiDAR) information. An example of DSM application can be found in (Redweik et al., 2013), where the authors exemplary analysed the University Campus of Lisbon (Portugal) to test the capability of their SOL algorithm in estimating solar irradiances on roofs and facades at 1 m spatial resolution and 1 h time step. On

* Corresponding author.
E-mail address: r.yao@reading.ac.uk (R. Yao).

https://doi.org/10.1016/j.jclepro.2018.02.139

the other hand, LiDAR technology has been recently employed by (Martínez-Rubio et al., 2016) in obtaining a detailed map of solar radiation for roofs and facades of an urban area approximately 80 km^2 wide in Spain using 5 mins irradiance records. More examples, together with a discussion of the strengths and limitations of different approaches employed to appraise the solar potential of an urban area, can be found in Section 2.1.

Despite several researchers have focused on the topic, not many have tackled the issue of understanding the matching issues between BIPV electricity production and buildings energy demand at the cluster level: Brownsword et al. (2005) estimated the PV resource for roofs application in Leicester city (UK) considering south, south-west and south-east orientations, fixing the suitable installation area at 75% of total roofs area and a module efficiency of 10%. Electricity demand data is gathered from two different local sources for an entire year at half-hourly time step.

Similarly, Lund (2012) analysed potential applications of PV panels on roofs for the two very different climates of Shanghai (China) and Helsinki (Finland) assuming 50% availability of roofs area and neglecting the shading effects. He also proposed different electricity management strategies, finding that for both the cities analysed electricity-to-thermal conversion of surplus renewable electricity (i.e. that beyond the self-use of consumers) outperforms electricity-to-storage and load-renewable production peak matching. Energy demand data is modelled by using a load distribution function exponentially declining when moving from the city centre to the outskirts.

More recently, Wegertseder et al. (2016) developed a method that combined solar mapping of roof surfaces carried out within a GIS environment with energy consumption patterns of the building stock in Concepción (Chile) modelled running dynamic simulations in DesignBuilder. Through the definition of typical buildings, the authors were able to develop different load profiles to be matched with the expected local electricity production and thus to predict the spatial power flows in the urban electricity grid.

Finally, (Brito et al., 2017) carried out a techno-economic analysis of the feasibility of BIPV in two different areas in Lisbon (Portugal) by coupling LiDAR and Typical Meteorological Year (TMY) weather data with the SOL algorithm proposed by (Redweik et al., 2013). Although accurate on the supply side, the demand side is estimated by means of a top-down approach by multiplying the estimated number of inhabitants by average per capita electricity demand. Different scenarios in terms of energy demand, such as the application of energy conservation measures or different occupancy patterns, cannot be addressed and would rather need a bottom-up approach (Reinhart and Cerezo Davila, 2016).

The aim of this paper is to develop a comprehensive bottom-up approach for helping local authorities, institutions and engineers understanding the technical potential of BIPV installations at the scale of cluster of buildings.

To this aim, a workflow has been implemented within the Python-based algorithm editor Grasshopper that interlinks state of the art modelling tools, local climate variables and daylight parameters in order to: i) estimate the energy demand of the institutional buildings by means of hourly dynamic simulations, ii) rank every surface according to a detailed solar radiation analysis accounting for both the direct and indirect solar radiation components and iii) appraise the BIPV yield achievable by the best surfaces.

In this way, the effect of different supply/demand strategies at the scale of clusters of buildings can be accounted for, thus greatly helping translate in practice the generic and nation-wide renewable production and energy efficiency goals set by laws and regulations.

2. Methodology

The proposed methodology makes use of detailed dynamic simulations to estimate both the electricity yield from BIPV installed on buildings envelopes (roofs and facades), and the buildings energy demand. The conceptual framework of Fig. 1 summarizes the main steps of this process: on the supply side, the solar radiation analysis of buildings surfaces allows to rank them according to the amount of solar radiation perceived in a year, and then to quantify the area available for PV installation according to an user-defined radiation threshold. Then, the electricity yield is estimated by considering also the environmental variables affecting the electrical efficiency of PV panels. On the demand side, the characterization of the buildings in terms of function, constructions, occupancy profiles and HVAC systems allows to get the energy demand profiles for various end-uses and thus their final electricity demand.

It is finally possible to compare both the supply and demand profiles in order to study the feasibility of different renewable share scenarios, as well as the matching issues arising from the use of a discontinuous energy source like the sun.

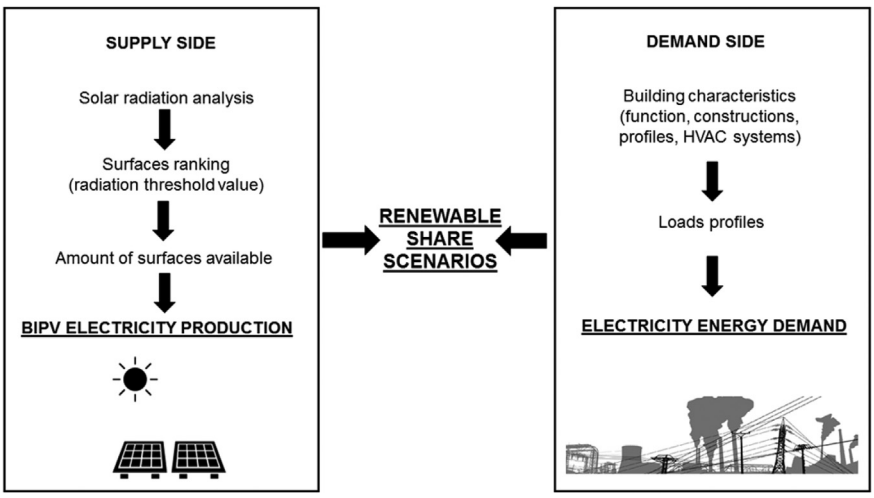

Fig. 1. Framework of the proposed methodology.

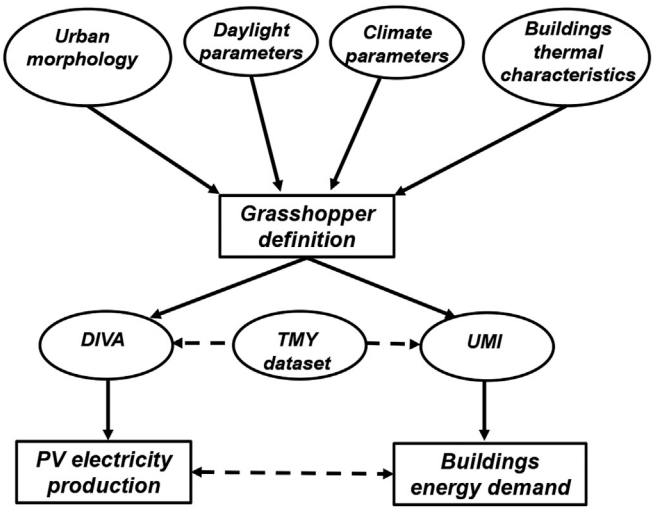

Fig. 2. Data interconnection among the different simulation tools.

To accomplish these tasks, several simulation tools are interconnected using the algorithm editor Grasshopper (see Fig. 2) that allows the users to write their own Python-based definitions. In our approach it is used to reference: i) a 3D model of the study area, ii) materials optical properties and sky conditions to run surface irradiance analysis (daylight parameters), iii) climatic parameters related to the specific site in the format of TMY dataset) and iv) building thermal characteristics to run dynamic energy simulations. The outputs generated by the different simulation tools are solar irradiation values for each surface of the model (DIVA software), PV efficiency values and electricity production for the best collecting surfaces (Grasshopper definition), and finally the energy needs of the buildings (UMI software).

Details for each modelling step outlined above are provided in the next subsections.

2.1. 3D model generation and irradiance analysis

In order to perform a quick analysis of the solar potential of a study area, a 3D model built at Level of Detail 1 is employed. According to (Biljecki, 2013), buildings at this level of detail are represented as footprint extrusions and with flat roofs. Nonetheless, it is possible to use more detailed three-dimensional representations for analysis concerning a limited number of buildings since computation time exponentially increases with the number of modelled surfaces.

Once the physical model is available, two main approaches for estimating solar irradiance values on building envelopes can be employed according to the literature review of Freitas et al. (2015): empirical based or computational based.

The *empirical based models* transpose the global and diffuse horizontal radiation values measured from weather stations located in open fields into the direct beam and diffuse components for any tilted surface by also considering the reflections due to the ground's albedo.

In general, there is a big consensus around the use of the Perez anisotropic sky model (Perez et al., 1987) that considers one direct beam component from the sun, three diffuse sky components – deriving from the circumsolar disc close to the sun's position, the horizon band close to the ground and the isotropic contribution from the remaining of the sky dome respectively – and the ground reflected component. However, these models fail when complex urban layouts need to be taken into account, especially when obstructions to sunlight can strongly affect solar harvesting like within dense urban environments. Consequently, the development of *computational based models* that mainly differ each other for the resolution (both spatial and temporal) of the analysis and the radiation components taken into account.

Most of the computational based models available in the literature focus on the appraisal of the direct and diffuse components only: Erdélyi et al. (2014) developed a vectorial-based model called SORAM that augments the anisotropic Perez sky formulation but is only applicable for flat/tilted roofs. Another vectorial model, based on 2.5D GIS geometric data of an urban area of Madrid (Spain), has been developed by Esclapés et al. (2014) and it is able to predict if the study points on both roofs and facades are sunlit by means of algebraic and trigonometric equations. The most detailed models developed so far, i.e. those able to account also for the reflected solar radiation component, made use of different approaches and calculation tools.

As an example, De La Flor et al. (De La Flor et al., 2005) developed a characterization method that relies on the use of an isotropic sky and fixed sun positions for getting irradiance values on surfaces (roofs and facades) assumed as grey bodies after that a fixed number of rays cast them according to a deterministic directional distribution.

Compagnon (2004) developed a computer program that used a 2.5D model to be translated into the Radiance format for running a detailed irradiance analysis on both roofs and facades. This approach has been tested for a district located in Fribourg (Switzerland), using the Perez sky formulation and a fixed value for the solar reflectance of every building surface.

Then, Jakubiec and Reinhart (2013) enhanced the Radiance based approach by coupling a detailed 3D GIS model of the city of Cambridge in the US – derived from LiDAR data – with DAYSIM irradiance hourly simulations. Their approach proved to be very detailed since a comparison with two existing rooftop installations showed annual errors less than 5% in terms of electricity production. However, only roofs are considered in this work.

The approach used in this study is computational based and furthers that of Jacubiec and Reinhart (Jakubiec and Reinhart, 2013) by using the capabilities of Radiance coupled with the visual interface provided by DIVA (Reinhart et al., 2014) to estimate solar irradiance values not only on roofs but also on building facades. Radiance is a well validated backward ray tracer tool (Ward and Rubinstein, 1988) that can use several sky models, from customized ones to standard CIE models. Because of this capability, hourly climate-based daylight simulations are carried out using the daylight coefficient approach implemented by Mardaljevic (2000) for the already mentioned Perez's sky model (Perez et al., 1987).

Another noticeable difference between the approach implemented here and that of (Jakubiec and Reinhart, 2013) is given by the use of a 3D model built within the Rhino CAD environment. Rhino is a powerful tool that allows modelling geometries of every complexity as well as to import different file formats and convert them into the .3 dm proprietary format. This means a high user flexibility because it is possible to import a physical model already available in other formats as well as to create a new one, thus bypassing the need for a GIS model that very often is available only for few big cities in the world.

The model is then referenced as a closed boundary representation (*brep*) and passed to Grasshopper where every surface is manipulated and characterized by assigning different optical and thermal properties.

Finally, the results of the simulations are shown in a false-colour scale showing both the amount of solar energy perceived by every surface as well as the extent of the surfaces receiving more than a

user-defined threshold value. This will greatly help in highlighting the best surfaces for PV panels' installation, for which the calculation of the electricity production detailed in the following can be performed.

2.2. PV panels' efficiency and electricity yields calculation

In the literature, several approaches have been employed for estimating PV efficiency variations due to different panel technologies (Mono-c-Si, Multi-c-Si, a-Si, CIGS, CdTe), mounting layout (i.e. free racks, roof mounted, building integrated) and operational conditions.

As reported by (Mattei et al., 2006), the most used model is represented by the following algebraic equation:

$$\eta_{PV} = \eta_{ref}\left[1 - \beta\left(T_c - T_{ref}\right) + \gamma LogI\right] \quad (1)$$

where the electrical efficiency η_{PV} is related to the reference value η_{ref} provided by the manufacturer under Standard Reporting Conditions (SRC), that is to say $T_{ref} = 25\,^{\circ}C$ and a solar irradiance value $I_{ref} = 1000\,W\,m^{-2}$ impinging on the panel surface (the G 173 solar irradiance spectrum distribution is usually used (ASTM G173-03, 2012). β and γ are the efficiency correction coefficients for cell temperatures and irradiance levels others than the standard ones, respectively, and depend on the material used for making the panel.

As an indication, β ranges from $-0.25\%^{\circ}C^{-1}$ for CdTe panels to $-0.45\%^{\circ}C^{-1}$ for Multi-c-Si panels, while γ ranges from 0.085 for Mono-c-Si installations to 0.12 for Multi-c-Si ones.

The previous equation is usually simplified by neglecting the explicit irradiance term $\gamma LogI$ without losing accuracy since the irradiance effect is implicitly taken into account by the cell temperature T_c.

An established way to obtain T_c (°C) via an energy balance on the module makes use of the so-called Nominal Operating Cell Temperature (NOCT). It is defined as the panel temperature reached under Nominal Terrestrial Environment (NTE) conditions, let's say global solar irradiance $I = 800\ Wm^{-2}$, ambient temperature $T_a = 20\,^{\circ}C$, average wind speed of 1 ms^{-1} (without considering any wind direction), no electrical load and free rack installations facing normal to noon. Under these conditions, the cell temperature can be expressed as:

$$T_c = T_a + (NOCT - 20)\frac{I}{800} \quad (2)$$

Again, NOCT values depend on the material used for making the panels and span from 43 °C for Mono-c-Si types to 47 °C for CIGS ones. However, this equation is rigorously applicable only to free rack installation, and cannot be used for BIPV applications as for this study. In fact, since the two sides of the modules experience quite different ambient conditions, new prediction approaches have to be sought.

If focusing on PV installations on building facades, the problem is further complicated by the nature of the environment surrounding the facades that alters the wind flow pattern and thus the magnitude of the heat exchanged by convection.

The determination of these losses is usually accounted for either by using convection heat transfer coefficients that are experimentally or theoretically derived (a thorough review of wind convection coefficient correlations useful for building envelope calculations is provided in (Palyvos, 2008)) or by running Computational Fluid Dynamics (CFD) analyses, the last ones being too time consuming and easily prone to errors to be carried out at urban scale.

Schwingshackl et al. (2013) tested eight different models to specifically predict cell temperatures, and found out that it is not possible to identify just one model able to accurately calculate panel temperatures and their efficiency under different operating conditions. However, the models including wind speed as a variable generally report better agreement with experimental measurements.

A detailed formulation accounting for air forced convection, natural convection and radiation losses in free standing PV installations has been developed by Kaplani and Kaplanis (2014) and allows to predict the cell temperature as a function of the ambient temperature and incident solar radiation on the panel:

$$T_c = T_a + fI \quad (3)$$

Here, f is an empirical coefficient, already addressed by other authors and firstly introduced by Ross (1976), which is estimated in relation to the overall heat losses of the panel.

An accurate and easy to use extension of this approach to BIPV installations in urban environments is that provided in ref. (Skoplaki et al., 2008): first, a mounting coefficient ω is defined as the ratio of the Ross' parameter for the specific mounting arrangement to that valid for the free rack case (the values taken by the mounting coefficient range from 1 for freestanding installations to 2.6 for façade-integrated installations):

$$\omega = \frac{f_{mounting}}{f_{free\_rack}} \quad (4)$$

Then, the wind convection coefficient is computed by making use of the well-known Loveday-Taki relation (Loveday and Taki, 1996):

$$h_w = 8.91 + 2.0v_f \quad (5)$$

and finally the cell temperature is estimated by the following equation:

$$T_c = T_a + \omega\left(\frac{0.32}{8.91 + 2.0v_f}\right)I \quad (6)$$

This relation holds for every mounting type and for free wind velocities v_f, that is to say those got by measurements taken at a mast-mounted anemometer well above the PV array.

The method developed in this paper makes use of Eq. (6) to estimate cell temperature values but slightly modifies it to account for the effect of the urban environment in lowering the wind speeds as gathered from meteorological datasets provided in the TMY format (Wilcox and Marion, 2008). This task is accomplished by using the traditional power law formulation (ASHRAE, 2005) and defining an urban-scaled wind velocity v_f^* (ms^{-1}):

$$v_f^* = v_{met}\left(\frac{\delta_{met}}{z_{met}}\right)^{\alpha_{met}}\left(\frac{z}{\delta}\right)^{\alpha} \quad (7)$$

Here, v_{met} and z_{met} are respectively the wind velocity and the height above the ground (typically 10 m) of the local weather station, z is the height for which the calculation is performed and δ and α are the boundary layer thickness and local terrain exponent coefficients. Typical values for the last ones are provided in (ASHRAE, 2005).

Finally, by combining Eq. (1) with Eq. (6) and considering also the losses due to power mismatch among the panels and those due to inverter operation by means of the mismatch and inverter efficiencies η_m and η_{inv} (their values are typically around 0.97 and 0.95 respectively and are provided by the manufacturers), the electrical yield of the effective PV panel collecting area A_{eff} is calculated at an

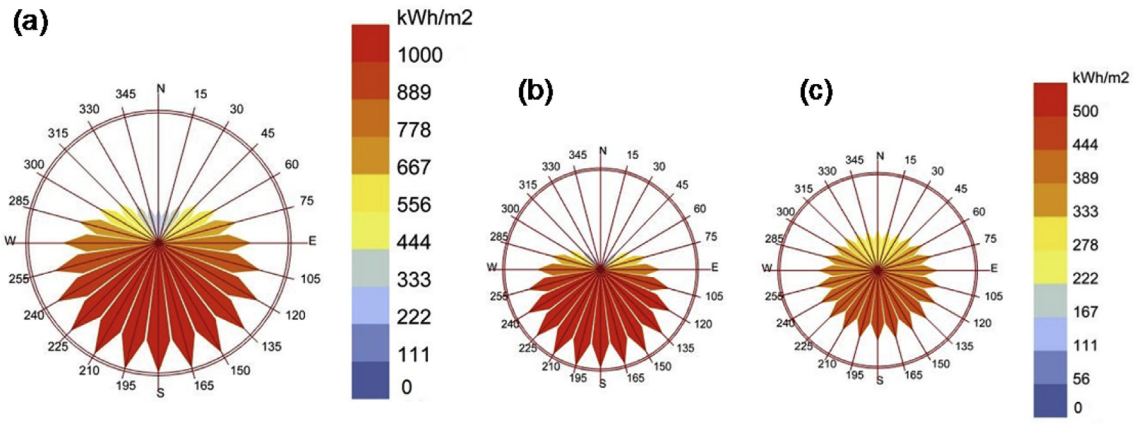

Fig. 3. Radiation roses for Izmir: (a) total radiation, (b) direct radiation and (c) diffuse radiation.

hourly time step with the following relation:

$$P = \eta_{PV}\eta_m\eta_{inv}A_{eff}I \quad (8)$$

2.3. Buildings' load profiles calculation

It is frequent the case when detailed data about the energy demand of buildings, in terms of hourly profile and breakdown of its components (cooling, heating, lighting and other equipment), is neither available nor practical to obtain. In such cases, especially at the scale of clusters of buildings, it is convenient to rely on dynamic thermal simulations to get this comprehensive information.

The devised methodology define buildings' load profiles by means of detailed dynamic simulations carried out using a recently-developed Urban Modelling Interface (UMI) (Reinhart et al., 2013) that has EnergyPlus v8.1 (US Department of Energy, 2017) as its core engine.

By referencing the same 3D urban model created for the solar irradiation analysis, the tool asks for all the data needed for running traditional EnergyPlus simulations: construction details, occupancy schedules, internal gains and HVAC characteristics. This piece of information is then attached to every building as a template. The burden of collecting all the data needed is counterbalanced by reduced simulation times, since UMI uses an algorithm able to split the buildings into representative thermal zones according to the definition of perimeter and core zones reported in the ASHRAE 90.1 Appendix G (ANSI/ASHRAE, 2002). The details of this procedure can be found in (Dogan et al., 2015), where validation tests show mean percentage errors between 2 and 5% when the annual energy demand is compared against the results of traditional EnergyPlus whole-building simulations.

The benefits are a strong reduction of simulation times that allows considering a big number of buildings in the analysis, and the capability of outputting detailed hourly profiles of the energy demand split into its heating, cooling, lighting and equipment components for every single building. Although the software itself reports on the electricity demand, it is possible to consider different energy vectors by inputting the appropriate energy conversion efficiencies so that different scenarios can be easily appraised (e.g. the choice between gas-fired boilers or heat pumps for space heating).

3. Implementation of the developed method – a case study at Yasar University

This section demonstrates the method for the case study of the Yasar University Campus in Izmir (Turkey). First, an overview of the local climate characteristics and campus layout is given, then calculations are performed for all the buildings and the outcomes of the modelling including one exemplary case will be discussed.

3.1. Yasar University case study

Izmir is a city located in the western coastline of Turkey (LAT 38°30′N, LON 27°1′E) that faces the Aegean Sea and whose climate

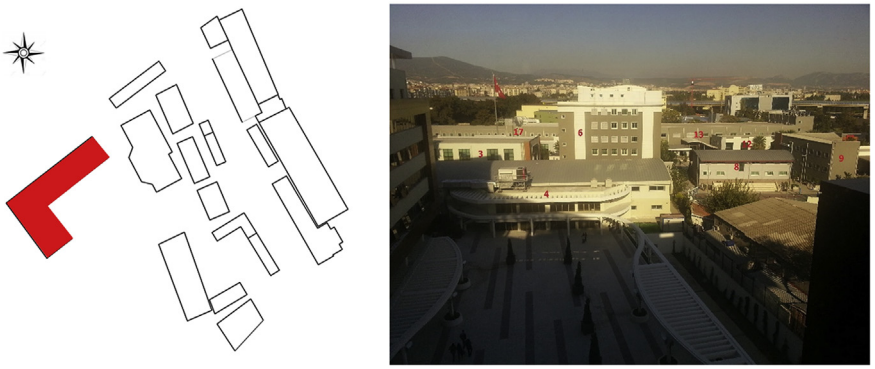

Fig. 4. Plan view of the campus with the test building highlighted in red (on the left) and frontal view of some of the campus buildings (on the right). (For interpretation of the references to colour in this figure legend, the reader is referred to the Web version of this article.)

Table 1
Radiance parameters.

ab	*ad*	*as*	*ar*	*aa*
3	1000	20	300	0.1

is classified as warm-humid according to ASHRAE Standards 90.1–2004 and 90.2–2004 (ASHRAE, 2004a,b), with 1408 HDD and 983 CDD annually calculated on a baseline of 18.3 °C (ASHRAE, 2009).

Daily average outdoor temperatures are around 25 °C in summer (June to September) and 10 °C in winter (December to February), while the corresponding average relative humidity values are 55% and 73% respectively. For what concerns solar radiation, the highest global radiation values are reached by surfaces exposed due south within ±45° tolerance, the main contribution being that of the direct radiation component (see radiation roses in Fig. 3).

The Yasar University Campus, located in the Bornova district, is made up of 18 buildings used for academic purposes (classrooms, offices, recreational services) while other buildings are used for hosting mechanical devices and other equipment. Fig. 4 shows a plan and frontal view of the campus buildings, with highlithed in red the building chosen for further detailed analysis. This building hosts classrooms that are usually occupied by students from 8:30 a.m. to 6:30 p.m., whereas offices are used by staff members from 8:30 a.m. to 5:30 p.m., Monday to Friday. Electricity consumption due to internal lighting and variuos equipments (printers, desktop computers and other amenities) amounts to 8 Whm^{-2} and 24 Whm^{-2} respectively.

The low energy demand for heating is delivered by gas-fired boilers, whereas a chiller with an average coeffiecient of performance of 4.86 provides space cooling. As for the constructions, metal sandwich panels filled with rockwool insulation are used for both the external walls (U-value of 0.35 $Wm^{-2}K^{-1}$) and the roof (U-value of 0.5 $Wm^{-2}K^{-1}$). Windows are double-glazed aluminum framed with an air gap and an external reflective coating (visible transmittance value of 0.57) with a resulting U-value of 2.8 $Wm^{-2}K^{-1}$.

3.2. Solar availability analysis and expected BIPV electricity yield from facades

Annual simulations have been performed in order to evaluate the amount of solar radiation impinging on each surface of the buildings at an hourly time step using the DIVA software (DIVA, 2017). In order to keep a good spatial resolution within reasonable simulation times, a mesh dimension of 1.5 × 1.5 m^2 has been chosen for the sensor nodes placed on the surfaces with their normal facing outwards. The solar reflectance values of ground, facades and roofs are set to 0.20, 0.35 and 0.30 respectively. As for the Radiance parameters, preliminary sensitivity analysis allowed to choose the values listed in Table 1 for running the simulations. In particular, higher ambient bounces (*ab*) values have been explored to assess their influence on the reflected component calculation. This exercise demonstrated that using higher *ab* values (up to 5)

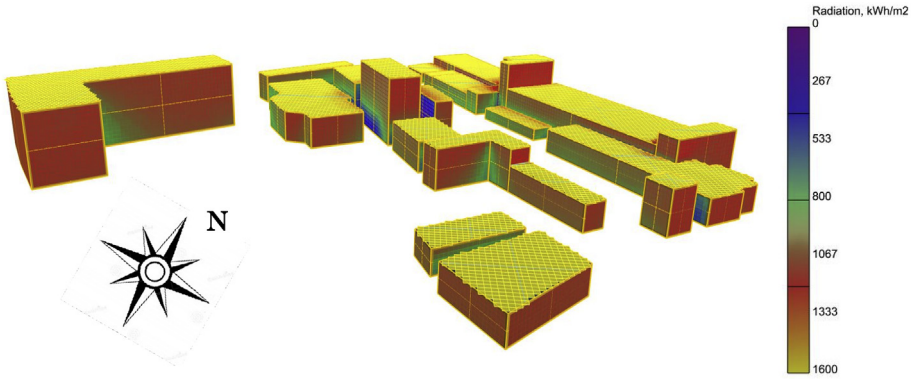

Fig. 5. Annual cumulative solar radiation values for the campus buildings.

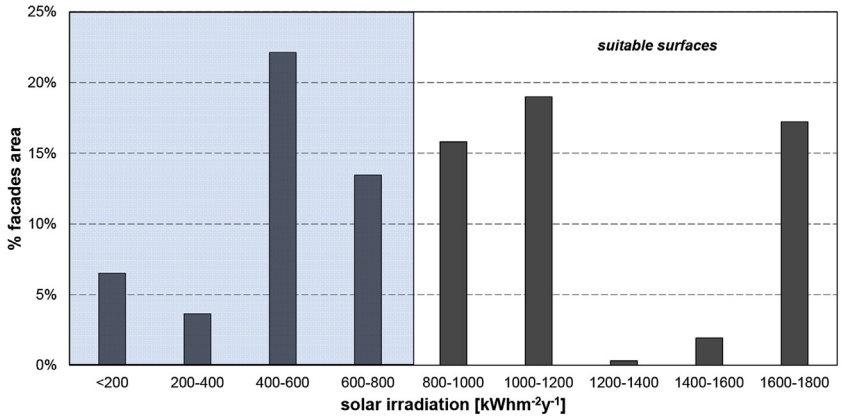

Fig. 6. Ranking of facades area according to the perceived annual solar radiation.

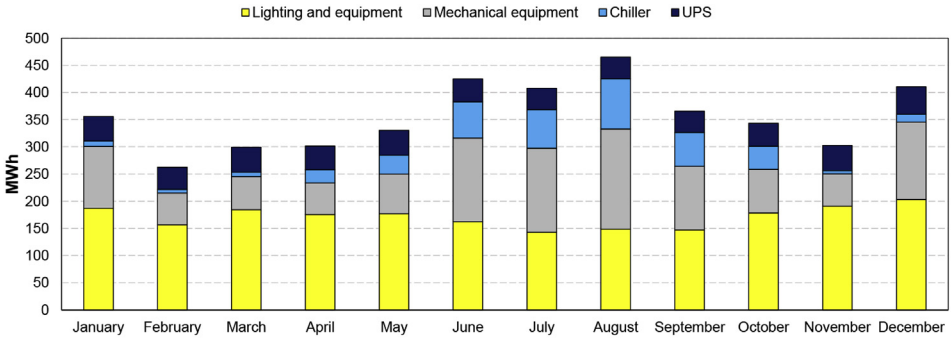

Fig. 7. Measured monthly electricity consumption of the campus.

would lead to negligible differences in the estimated annual perceived radiation (less than 5%), but at the expense of much higher simulation times (up to three times).

Simulations have been carried out also by neglecting the reflected component ($ab = 0$); in this case, differences up to minus 60% could be expected in the amount of the solar radiation perceived by surfaces shaded by the surroundings, irrespective of their orientation. This rebates the need for a detailed radiation analysis that accounts for reflections among several facades within an urban environment.

Finally, annual cumulative solar radiation values have been plotted on the 3D model of the campus as surface-averaged values on a false-colour scale with the aim of showing the most suitable surfaces for BIPV application.

From this analysis (see Fig. 5) it emerges how, apart from the mutual shading effects due to the buildings layout, the most suitable vertical surfaces are those facing the south/south-west directions.

However, not all of these facades (around 21 720 m^2) are adequate to host PV panels: in order to rank them, a solar radiation threshold value needs to be defined. According to Compagnon (2004), this threshold has been set to 800 $kWhm^{-2}y^{-1}$, making the potential surfaces amount equal to 11 790 m^2 (i.e. the sum of the suitable surfaces listed in Fig. 6 according to their perceived solar radiation).

Further reductions have to be considered for accounting of windows, protrusions or technical services that limit PV applications to facades: the only reference value found in the literature suggests a 20% reduction due to balconies and alcoves (Fath et al., 2015). This value has been incremented up to 50% for considering also the space occupied by windows, assuming a fixed window to wall ratio of 0.3. In the end, the amount of facades that are suitable for BIPV installations equals to 5895 m^2, which represent 27% of the total facades area. By using the technical specifications for the photovoltaic panels installed on the same exemplary building of this study by Shahrestani et al. (2017), the expected annual electricity delivery from BIPV panels on facades only has been calculated using Eq. (8) and amounts to 1010 MWh. This equals to a reduction in carbon emissions of approximately 495 tCO_2, as calculated according to the carbon emission factor reported in (Turkey energy efficient report, 2011).

3.3. Buildings energy demand

University campus management staff measured the electricity consumption due to interior/exterior lighting, appliances and mechanical equipment for all the campus buildings on a monthly basis throughout the year 2016 from the local electricity transformer. These values are reported in Fig. 7, and amounts to an annual consumption of 4270 MWh, thus making the share of electricity needs that can be annually supplied by BIPV under the business as usual scenario around 23%.

This result is considered very positive since it allows to comply with the Renewable Energy Directive that prescribes, among the others, to cover at least 20% of the energy needs by means of renewable sources by 2020 (European Parliament, 2009). However, if more ambitious scenarios should be implemented by considering electricity production from PV panels only, additional suitable

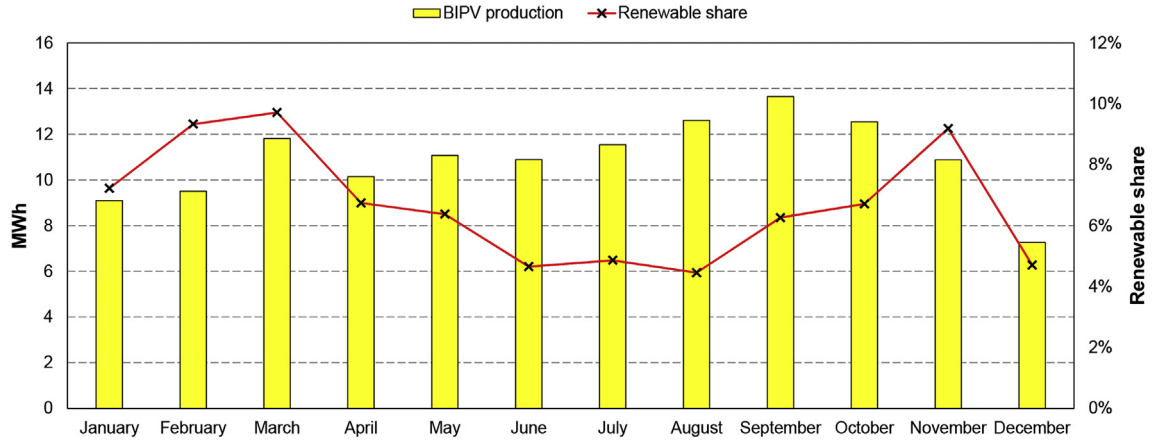

Fig. 8. Monthly BIPV electricity production (yellow bars) and share of energy demand (red line) covered by BIPV for the test building. (For interpretation of the references to colour in this figure legend, the reader is referred to the Web version of this article.)

surfaces may be sought. In this sense, roofs represent the most obvious choice because of the large amount of surfaces available and of the higher radiation values reached as shown in Fig. 5. Nonetheless, it is worth to mention that surface reductions should be considered as well for installations on flat roofs, especially when other green building strategies such as green roofs have to be accommodated (Tong et al., 2016).

3.4. Demand and supply matching for an exemplary building

A finer level of detail at both spatial and temporal scales is needed when dealing with the energy supply from discontinuous energy resources such as solar and wind in order to predict with reasonable accuracy the matching issues between energy supply and demand.

The proposed method allows reaching a temporal resolution of 1 h on both the supply and demand side calculation steps. Based on the monthly measured energy consumption of the campus previously discussed, a calibrated energy model of the campus buildings has been developed in UMI making use of the same 3D model built for the irradiation analysis.

For the sake of showing the importance of considering simultaneously both the single building scale and that of clusters, the matching issues are here discussed for the exemplary building highlighted in Fig. 4. This building mainly hosts classrooms throughout the year and it is the most energy consuming of the campus, with a monthly peak electricity consumption of around 14 MWh in September (see Fig. 8). According to the solar radiation analysis carried out previously, a suitable area of 1302 m^2 could be successfully used for BIPV application, which leads to the monthly renewable shares (i.e. the share of the total electricity demand deliverable by photovoltaics) depicted in Fig. 8 on the secondary y-axis. This monthly supply profile shows that the peak electricity production from BIPV occurs from August to October, because of the higher solar radiation values and of the more favourable solar height. Nevertheless, the maximum renewable share achievable is around 10%, meaning that the remaining electricity demand has to be delivered by the grid or by an oversupply from other buildings of the same cluster.

A way to better exploit the electricity production potential from BIPV could thus be that of covering just one or more final energy uses. A breakdown of the electricity demand showed that electrical equipment, including plug loads and artificial lights, have a magnitude comparable to that of BIPV electricity yield in terms of kWh. Fig. 9 shows the hourly profiles of the energy demand for electrical equipment (blue line) and of the BIPV electricity production (orange line). According to the monthly supply profile discussed above, peak power production occurs when the solar height is more favourable, i.e. during summer and transition months, but of course it shows a discontinuous trend. On the other hand, energy uses related with electrical equipment keep almost constant throughout the year. In fact, a three-step profile characterizes weekdays (around 8 kWh from 10 p.m. to 7 a.m., up to 80 kWh from 8 a.m. to 6 p.m. and down to around 50 kWh from 7 p.m. to 9 p.m.), while a constant demand of 8 kWh can be assumed for the weekends when just some equipment is on stand-by mode (see Fig. 9).

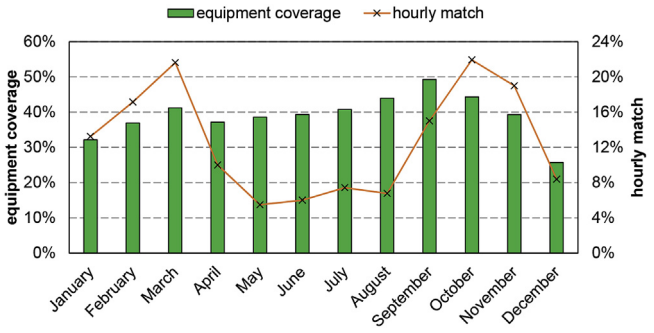

Fig. 10. Monthly equipment demand coverage (bars) and hourly matching occurrences (line) for the test building.

From this hourly representation, it is easy to notice how seldom the peak demand is matched by BIPV. A finer analysis of the matching issues is reported in Fig. 10 where the monthly coverage of the equipment demand from BIVP (green bars, primary y-axis) is plotted against the percentage of hourly matching per month (orange line, secondary y-axis), calculated during the period 8 a.m. to 6 p.m. in order to not account for those hours without solar radiation. The outcomes of this analysis show that, in spite of monthly coverage values up to 50% (in terms of cumulative electricity demand and supply), BIPV can effectively match the equipment demand on an hourly basis for less than 22% of the time under peak production conditions.

The resolution provided from the simulation framework

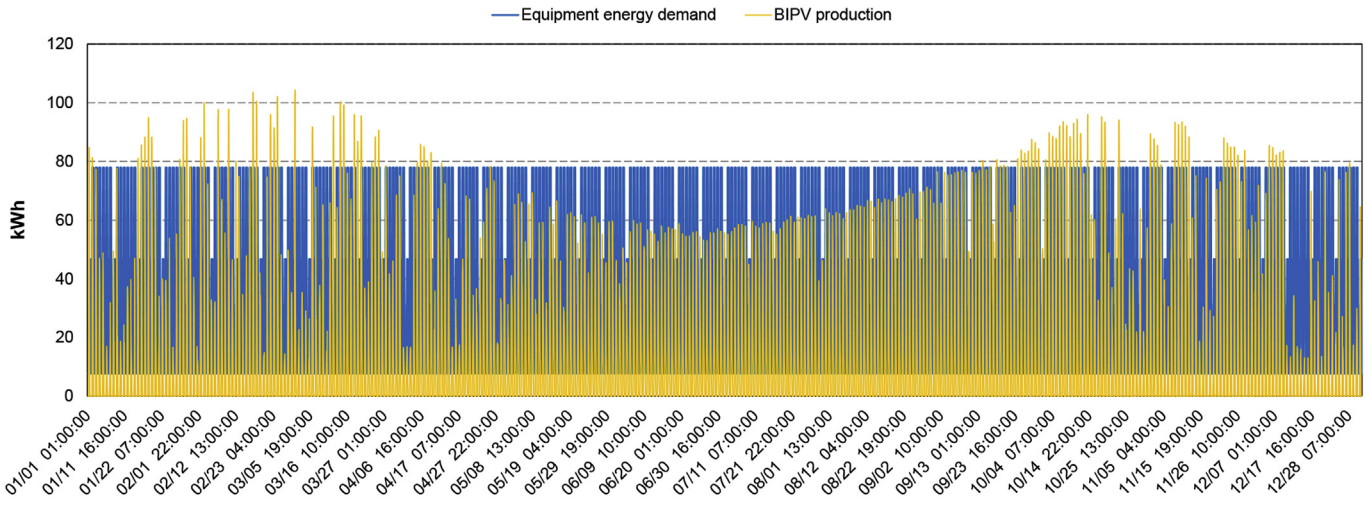

Fig. 9. Hourly equipment energy demand and BIPV electricity production of the test building.

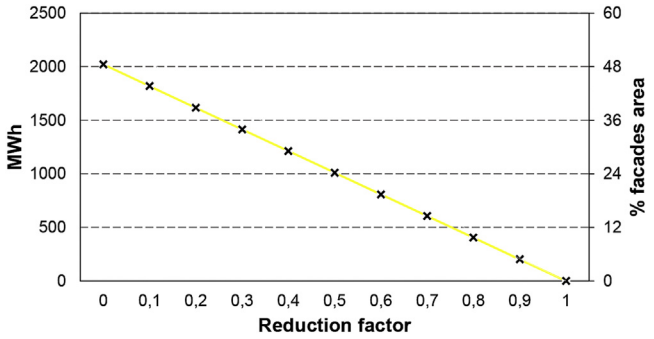

Fig. 11. Electricity yield as a function of reduction factor and resulting facades area share.

developed can then inform about the adoption of different strategies such as i) supply from the grid, ii) BIPV supply from nearby buildings and iii) adoption of a storage system (to be designed according to a carefully chosen electricity demand threshold to avoid oversizing and malfunctioning).

4. Discussion

The method introduced in this paper first helps identifying and quantifying the amount of facades area deemed suitable for PV installation according to an annual solar radiation threshold. In the literature, there is a wide consensus around the adoption of the values suggested by Compagnon (2004) for both facades (800 $kWhm^{-2}$) and roofs (1000 $kWhm^{-2}$) because they reflect the technological features of photovoltaic panels currently available on the market. Nevertheless, by analysing Fig. 6, it is possible to estimate the variation of the suitable surfaces amount due to the adoption of different irradiation threshold values. As an example, a decrease of this value from 800 $kWhm^{-2}$ to 600 $kWhm^{-2}$ due to technological improvements leads to an increase in the suitable facades area of around 7%, and to a renewable share of around 27% against the original value of 23%. Although not negligible, this difference is less than 5% and no significant improvements in the electricity yield are expected when changing the solar radiation threshold to a reasonable lower or higher value. On the contrary, changes in the reduction factor of facades due to real urban morphology, geometric and technical constraints strongly affect the expected electricity yield: the sensitivity analysis carried out in Fig. 11 shows a linear relationship with a slope of around −20 MWh per percent increase of the reduction factor. These differences, apart from being site-related, also depend on the level of detail of the 3D model of the study area: the finer the model, the bigger is the accuracy in the electricity yield estimate and the lower the need to rely on reduction factors.

Moreover, it is worth to mention how the optical properties (solar reflectance values namely) used for characterizing the urban surfaces are typical of highly urbanized contexts (see Section 3.2), and are not expected to affect the outcomes of the calculations in a significant way. However, under particular circumstances - such as when the buildings are surrounded by green areas, water surfaces or by glazed surfaces - these parameters should be changed accordingly.

Finally, it is important to state that an economic analysis of the investment profitability is out of the scopes of this paper. The reader can refer to the work of (Cucchiella et al., 2015) for a comprehensive technical-economic analysis involving the use of several indicators (net present value, internal rate of return, discounted payback period, discounted aggregate cost-benefit ratio and reduction of carbon dioxide emissions namely), and to that of (Kim et al., 2017) for the optimal installation timing of BIPV when considering variations in electricity prices.

5. Conclusions

This paper presents a comprehensive method intended to help institutional decision makers and engineers in addressing the technical feasibility of Building Integrated Photovoltaic (BIPV) applications for urban buildings. This bottom-up methodology advances current studies on the same topic by coupling state of the art simulation tools to allow a direct comparison between the electricity production from BIPV (supply side) and the energy needs (demand side) of urban buildings at a district scale and at an hour time step.

More in detail, after the creation of a three-dimensional representation of the study area, a detailed hourly-based solar radiation analysis is performed by means of Radiance simulations. The outcomes of this analysis are plotted in the model in order to show and quantify the most suitable surfaces for photovoltaic applications. Solar radiation values are then coupled with other environmental parameters derived from Typical Meteorological Year (TMY) dataset and processed in Grasshopper for estimating the electricity production from BIPV. Finally, thermal simulations using the EnergyPlus software are run for every study building in order to get the energy consumption profile. Comparison between supply and demands informs about the best strategy to adopt to achieve the targeted renewable energy shares.

The implementation of the method for the case study of Yasar University campus (Turkey) revealed that around 27% of façades area is suitable for BIPV installations. This leads to a renewable share cover, i.e. the amount of total annual electricity needs that can be supplied by photovoltaic, of about 23% under a business as usual scenario. This result is considered very positive and comply with the Renewable Energy Directive in force in Europe prescribing a 20% renewable share target by 2020. However, hourly matching issues between supply and demand of an exemplary building within the campus showed that only electrical equipment loads can be partially matched on an hourly basis (for around 22% of the time under peak production conditions namely). In such cases, the use of the devised method can help inform the choice of a suitable strategy to better exploit BIPV potentialities such as the supply from the grid or from nearby buildings, or the adoption of an energy storage system.

Acknowledgements

The presented work was developed within the framework of project 'REELCOOP - Research Cooperation in Renewable Energy Technologies for Electricity Generation', funded by the European Commission (FP7 ENERGY. 2013.2.9.1, Grant agreement no: 608466). The authors would like to thank Ms. Elena Rico, Mr. Juan Luis Lechón and Mr. Teodosio del Caño from Onyx Solar for their technical assistant.

Appendix A. Supplementary data

Supplementary data related to this article can be found at https://doi.org/10.1016/j.jclepro.2018.02.139.

References

ANSI/ASHRAE, 2002. ASHRAE guideline 14-2002 measurement of energy and demand savings. Ashrae 8400, 170.
ASHRAE Standard 90.1-2004, 2004a. Energy Standard for Buildings except Low-rise

Residential Buildings. ASHRAE, Atlanta.
ASHRAE Standard 90.2-2004, 2004b. Energy-efficient Design of Low-rise Residential Buildings. ASHRAE, Atlanta.
ASHRAE, 2005. ASHRAE Handbook - Fundamentals. Atlanta, GA, USA.
ASHRAE, 2009. ASHRAE Handbook Fundamentals, American Society of Heating. Refrigerating and Air-Conditioning Engineers, Inc., Atlanta.
ASTM G173-03, 2012. Standard Tables for Reference Solar Spectral Irradiances: Direct Normal and Hemispherical on 37° Tilted Surface.
Baljit, S.S.S., Chan, H.-Y., Sopian, K., 2016. Review of building integrated applications of photovoltaic and solar thermal systems. J. Clean. Prod. 137, 677–689. https://doi.org/10.1016/j.jclepro.2016.07.150.
Biljecki, F., 2013. The Concept of Level of Detail in 3D City Models – PhD Research Proposal. GISt Report No. 62. TU Delft. Accessed June 2017. http://www.gdmc.nl/publications/reports/GISt62.pdf.
Biyik, E., Araz, M., Hepbasli, A., Shahrestani, M., Yao, R., Shao, L., Essah, E., Oliveira, A.C., del Caño, T., Rico, E., Lechón, J.L., Andrade, L., Mendes, A., Atlı, Y.B., 2017. A key review of building integrated photovoltaic (BIPV) systems. Eng. Sci. Technol. an Int. J. 20, 833–858. https://doi.org/10.1016/j.jestch.2017.01.009.
Brito, M.C., Freitas, S., Guimaraes, S., Catita, C., Redweik, P., 2017. The importance of facades for the solar PV potential of a Mediterranean city using LiDAR data. Renew. Energy 111, 85–94. https://doi.org/10.1016/j.renene.2017.03.085.
Brownsword, R.A., Fleming, P.D., Powell, J.C., Pearsall, N., 2005. Sustainable cities - modelling urban energy supply and demand. Appl. Energy 82, 167–180. https://doi.org/10.1016/j.apenergy.2004.10.005.
Compagnon, R., 2004. Solar and daylight availability in the urban fabric. Energy Build. 36, 321–328. https://doi.org/10.1016/j.enbuild.2004.01.009.
Cucchiella, F., D'Adamo, I., Lenny Koh, S.C., 2015. Environmental and economic analysis of building integrated photovoltaic systems in Italian regions. J. Clean. Prod. 98, 241–252. https://doi.org/10.1016/j.jclepro.2013.10.043.
De La Flor, F.J.S., Cebolla, R.O., Félix, J.L.M., Domínguez, S.Á., 2005. Solar radiation calculation methodology for building exterior surfaces. Sol. Energy 79, 513–522. https://doi.org/10.1016/j.solener.2004.12.007.
DIVA software, 2017. Accessed June. http://solemma.net/Diva.html.
Dogan, T., Reinhart, C., Michalatos, P., 2015. Autozoner: an algorithm for automatic thermal zoning of buildings with unknown interior space definitions. J. Build. Perform. Simul 1493, 1–14. https://doi.org/10.1080/19401493.2015.1006527.
Erdélyi, R., Wang, Y., Guo, W., Hanna, E., Colantuono, G., 2014. Three-dimensional SOlar RAdiation Model (SORAM) and its application to 3-D urban planning. Sol. Energy 101, 63–73. https://doi.org/10.1016/j.solener.2013.12.023.
Esclapés, J., Ferreiro, I., Piera, J., Teller, J., 2014. A method to evaluate the adaptability of photovoltaic energy on urban fa?ades. Sol. Energy 105, 414–427. https://doi.org/10.1016/j.solener.2014.03.012.
EU, 2010. Directive 2010/31/EU of the European parliament and of the council of 19 may 2010 on the energy performance of buildings (recast). Off. J. Eur. Union 13–35. https://doi.org/10.3000/17252555.L_2010.153.eng.
European Parliament, 2009. Directive 2009/28/EC of the European parliament and of the council of 23 april 2009. Off. J. Eur. Union 140, 16–62. https://doi.org/10.3000/17252555.L_2009.140.eng.
Fath, K., Stengel, J., Sprenger, W., Wilson, H.R., Schultmann, F., Kuhn, T.E., 2015. A method for predicting the economic potential of (building-integrated) photovoltaics in urban areas based on hourly Radiance simulations. Sol. Energy 116, 357–370. https://doi.org/10.1016/j.solener.2015.03.023.
Freitas, S., Catita, C., Redweik, P., Brito, M.C., 2015. Modelling solar potential in the urban environment: state-of-the-art review. Renew. Sustain. Energy Rev. 41, 915–931. https://doi.org/10.1016/j.rser.2014.08.060.
iNSPiRe Project reports D2.1a-D2.1c, 2014. Survey on the Energy Needs and Architectural Features of the EU Building Stock. Last accessed: November 2017 http://www.inspirefp7.eu/about-inspire/downloadable-reports/.
Jakubiec, J.A., Reinhart, C.F., 2013. A method for predicting city-wide electricity gains from photovoltaic panels based on LiDAR and GIS data combined with hourly Daysim simulations. Sol. Energy 93, 127–143. https://doi.org/10.1016/j.solener.2013.03.022.
Kaplani, E., Kaplanis, S., 2014. Thermal modelling and experimental assessment of the dependence of PV module temperature on wind velocity and direction, module orientation and inclination. Sol. Energy 107, 443–460. https://doi.org/10.1016/j.solener.2014.05.037.
Kim, B., Kim, K., Kim, C., 2017. Determining the optimal installation timing of building integrated photovoltaic systems. J. Clean. Prod. 140, 1322–1329. https://doi.org/10.1016/j.jclepro.2016.10.020.
Loveday, D.L., Taki, A.H., 1996. Convective heat transfer coefficients at a plane surface on a full-scale building facade. Int. J. Heat Mass Tran. 39, 1729–1742.
Lund, P., 2012. Large-scale urban renewable electricity schemes - integration and interfacing aspects. Energy Convers. Manag. 63, 162–172. https://doi.org/10.1016/j.enconman.2012.01.037.
Mardaljevic, J., 2000. Day Light Simulation : Validation, Sky Models and Day Light Coefficients. PhD Research.
Martínez-Rubio, A., Sanz-Adan, F., Santamaría-Peña, J., Martínez, A., 2016. Evaluating solar irradiance over facades in high building cities, based on LiDAR technology. Appl. Energy 183, 133–147. https://doi.org/10.1016/j.apenergy.2016.08.163.
Mattei, M., Notton, G., Cristofari, C., Muselli, M., Poggi, P., 2006. Calculation of the polycrystalline PV module temperature using a simple method of energy balance. Renew. Energy 31, 553–567. https://doi.org/10.1016/j.renene.2005.03.010.
Palyvos, J.A., 2008. A survey of wind convection coefficient correlations for building envelope energy systems' modeling. Appl. Therm. Eng. 28, 801–808. https://doi.org/10.1016/j.applthermaleng.2007.12.005.
Perez, R., Seals, R., Ineichen, P., Stewart, R., Menicucci, D., 1987. A new simplified version of the perez diffuse irradiance model for tilted surfaces. Sol. Energy 39, 221–231. https://doi.org/10.1016/S0038-092X(87)80031-2.
Redweik, P., Catita, C., Brito, M., 2013. Solar energy potential on roofs and facades in an urban landscape. Sol. Energy 97, 332–341. https://doi.org/10.1016/j.solener.2013.08.036.
Reinhart, C., Rakha, T., Weissman, D., 2014. Predicting the daylit area—a comparison of students assessments and simulations at eleven schools of architecture. Leukos 10, 193–206. https://doi.org/10.1080/15502724.2014.929007.
Reinhart, C.F., Cerezo Davila, C., 2016. Urban building energy modeling - a review of a nascent field. Build. Environ. 97, 196–202. https://doi.org/10.1016/j.buildenv.2015.12.001.
Reinhart, C.F., Dogan, T., Jakubiec, J.A., Rakha, T., Sang, A., 2013. Umi - an urban simulation environment for building energy use, daylighting and walkability. In: Proc. BS2013 13th Conf. Int. Build. Perform. Simul. Assoc, pp. 476–483.
Ross, R.G.J., 1976. Interface design considerations for terrestrial solar cell modules. In: 1976 Photovolt. Spec. Conf, pp. 801–806.
Schwingshackl, C., Petitta, M., Wagner, J.E., Belluardo, G., Moser, D., Castelli, M., Zebisch, M., Tetzlaff, A., 2013. Wind effect on PV module temperature: analysis of different techniques for an accurate estimation. Energy Procedia 40, 77–86. https://doi.org/10.1016/j.egypro.2013.08.010.
Shahrestani, M., Yao, R., Essah, E., Shao, L., Oliveira, A.C., Hepbasli, A., Biyik, E., Caño, T., del, Rico, E., Lechón, J.L., 2017. Experimental and numerical studies to assess the energy performance of naturally ventilated PV façade systems. Sol. Energy 147, 37–51. https://doi.org/10.1016/j.solener.2017.02.034.
Skoplaki, E., Boudouvis, A.G., Palyvos, J.A., 2008. A simple correlation for the operating temperature of photovoltaic modules of arbitrary mounting. Sol. Energy Mater. Sol. Cells 92, 1393–1402. https://doi.org/10.1016/j.solmat.2008.05.016.
Tong, Z., Whitlow, T.H., Landers, A., Flanner, B., 2016. A case study of air quality above an urban roof top vegetable farm. Environ. Pollut. 208, 256–260. https://doi.org/10.1016/j.envpol.2015.07.006.
Turkey Energy efficient report, 2017. accessed November. https://library.e.abb.com/public/bcfe8957cb2c8b2ac12578640051cf04/Turkey.pdf.
US Department of Energy, 2017. EnergyPlus Version 8.1 accessed June. http://apps1.eere.energy.gov/buildings/energyplus/.
Ward, G.J., Rubinstein, F.M., 1988. A new technique for computer simulation of illuminated spaces. J. Illum. Eng. Soc. https://doi.org/10.1080/00994480.1988.10748710.
Wegertseder, P., Lund, P., Mikkola, J., García Alvarado, R., 2016. Combining solar resource mapping and energy system integration methods for realistic valuation of urban solar energy potential. Sol. Energy 135, 325–336. https://doi.org/10.1016/j.solener.2016.05.061.
Wilcox, S., Marion, W., 2008. Users manual for TMY3 data sets. Renew. Energy 51 doi:NREL/TP-581-43156.